JOURNAL OF MATERIALS SCIENCE 27 (1992) 637–640

Effect of plasma on nitriding of Fe–18Cr–9Ni alloy

H. KUWAHARA, H. MATSUOKA, I. TAMURA
Research Institute for Applied Sciences, Tanaka-Ohicho, Sakyo-ku, Kyoto 606, Japan
J. TAKADA
Department of Applied Chemistry, Okayama University, Tsushima-Naka, Okayama 700, Japan
S. KIKUCHI, Y. TOMII
Department of Metal Science and Technology, Kyoto University, Sakyo-ku, Kyoto 606, Japan

The plasma nitriding behaviour of Fe–18Cr–9Ni alloy was compared with gas nitriding. The alloy was nitrided under the following conditions: specimen temperature: 823 K, nitriding time: mainly 108 ks, total pressure: 0.4–0.7 kPa, mixture ratio of N_2 and H_2: 0.25, discharge voltage: 350–450 V, current: 0.8–1.1 A. Formation of a surface layer of iron nitrides was not observed. Formation of a homogeneous internal nitriding layer, consisting of small precipitates of CrN and the γ-phase matrix, was, however, noted. The lattice constant at the specimen surface was smaller than that at greater depth. This may have been because the sputtering effect decreased the dissolved nitrogen content at the specimen surface. The sputtering of iron nitrides at the specimen surface by the plasma was experimentally confirmed through γ′–Fe_4N formation on Si beside an alloy specimen. The characteristics of the plasma nitriding mentioned above are discussed in relation to the sputtering.

1. Introduction

The nitriding of iron or iron alloys is recognized as an important method of surface modification [1] and is carried out on a large scale in many industries. Nitriding imparts high fatigue strength, wear resistance, and corrosion resistance to the alloys [2]. However, conventional ammonia gas nitriding is not readily applicable to the nitriding of austenitic iron alloys with a high chromium content, such as Fe–18Cr–9Ni alloy. In this case, the surface chromium oxide film suppresses nitriding of these alloys.

Although removal of the surface oxide layer by acid solutions enables the gas nitriding of the alloys, the nitriding is heterogeneous below 873 K [3]. Recently, we pointed out that gas nitriding was also achieved by first reducing the oxide layer by heating in hydrogen gas [4]. Ammonia gas nitriding of Fe–18Cr–9Ni alloy at 823 K (550 °C) results in the formation of an external nitriding layer and an internal nitriding layer. The former layer consists of a thin ε-Fe_2N_{-3} layer, γ′-Fe_4N layer about 10 μm in thickness, and the precipitation of CrN, while the latter layer is formed with a matrix of austenitic phase and small precipitates of Cr_2N [4].

We found that plasma nitriding is an easy and reproducible process for nitriding austenitic steels, and obviates the need to remove the surface oxide layer even at temperatures below 823 K [5]. Plasma nitriding of Fe–18Cr–9Ni alloy below 823 K results in the formation of an internal nitriding layer containing small precipitates of CrN in a matrix of austenite phase from the specimen surface. No external nitriding layer is formed.

The behaviour of Fe–18Cr–9Ni alloy is thus markedly different in plasma nitriding from gas nitriding. The microstructure formed by plasma nitriding at 823 K is similar to that in austenitic iron alloys of Fe–Cr–Ni–Ti [6] and Fe–Cr–Ni [7] nitrided at high temperatures using an ammonia gas or a mixture of nitrogen and hydrogen.

There has, however, been no study to explain these differences between the two nitriding methods. Thus, the present study aims to obtain further details about the characteristics of the nitriding layers formed in the plasma and gas nitriding processes. Such information is necessary for clarifying the role of the plasma. For this purpose, the nitriding layers were carefully studied by microstructural observation, and the precipitates of chromium nitrides were examined by X-ray diffraction (XRD) analysis. The concentrations of dissolved nitrogen in the nitrided specimens were also discussed in terms of the lattice constant of the austenitic matrix phase determined by XRD.

2. Experimental procedure

Fe–18Cr–9Ni alloy was used in the present study since its chemical composition, shown in Table I, is representative of austenitic stainless steels. The specimens of $10 \times 10 \times 20\ mm^3$ were cut from bars that had been rolled and quenched in water from 1423 K (1150 °C). This is a solid solution heat treatment. The surface of

0022–2461/92 $03.00 + .12

each specimen was mechanically polished using a buff with alumina particles (0.3 μm in diameter) and cleaned in acetone using an ultrasonic cleaner. Though small amounts of a ferritic phase were detected after mechanical polishing, this ferritic phase was faded during heating in the range of 373–473 K (100–200 °C). Table II shows the plasma nitriding conditions. The specimens were connected to a cathode in a chamber, that was connected to an anode, with a potential equal to the ground. The plasma nitriding temperature was measured using a thermocouple inserted into a hole with a diameter of 3.3 mm in a dummy specimen that was positioned in a similar manner to the specimens to be nitrided. The temperature was controlled within ± 4 K during nitriding. A single Si crystal with orientation of ⟨1 0 0⟩ was also positioned beside the iron alloy specimens for the purpose of determining the formation of iron nitrides due to sputtering on the specimen surface. A small misfit, $\varepsilon = 0.013$–0.014, between Si (1 0 0) and γ'–Fe_4N (1 1 0) plane is significantly effective on the formation of γ'–Fe_4N (1 1 0) on Si without scuffing due to sputtering from the specimen surface.

For comparison, ammonia gas nitriding was also carried out at 823 K for 68.4 ks (19 h) after annealing in an atmosphere of reduced hydrogen [5]. Pre-annealing was conducted to eliminate the surface oxide layer; surface oxide layers which exist as, for example, Cr_2O_3, suppress the ammonia gas nitriding of stainless steel. The annealed specimens were cooled to room temperature in a reduced hydrogen atmosphere.

The nitrided specimens were carefully cut into halves parallel to the specimen surface. Their cross-sections were mechanically polished and etched in a corrosive solution (5 g $FeCl_2$ + 2 ml HCl + 96 ml C_2H_5OH). The appearance and thickness of the nitriding layers were then examined using an optical microscope equipped with a micrometer.

The X-ray diffraction technique was used to identify the nitride formed in the specimens, particularly for the specimens nitrided in an atmosphere of 25%N_2 and 75%H_2 at 823 K, using cross-sections cut at various distances from the specimen surface. CoK_α with Fe filter and CuK_α with Ni filter were used for Fe–18Cr–9Ni specimens and single Si crystal, respectively.

TABLE I Chemical composition of the specimen used (wt %)

C	Si	Mn	P	S	Cr	Ni	Cu
0.034	0.36	1.76	0.034	0.012	18.00	9.23	0.17

TABLE II Conditions of plasma nitriding

Specimen temperature	823 K
Nitriding time	108 ks
Discharge voltage	350–450 V
Discharge current	0.8–1.1 A
Ratio of gases	25%N_2 and 75%H_2
Total pressure	0.4–0.7 kPa

3. Results and discussion.

Fig. 1 shows the typical microstructure of Fe–18Cr–9Ni alloy plasma nitrided at 823 K (550 °C) for 108 ks (30 h), where *S* is the specimen surface, *F* the nitriding front, and *E* is the thickness of the nitriding layer. This figure clearly shows that the nitriding front advances parallel to the specimen surface and that no external nitriding layer can be observed. These facts suggest that lattice diffusion of nitrogen rather than diffusion at the grain boundary predominates in this alloy. In contrast to the formation of both an external and internal nitrided layers in a similar alloy nitrided using ammonia gas [5], the absence of the external layer is apparent in the plasma nitrided specimen. This absence of an external layer is the most notable characteristic of plasma nitriding of Fe–18Cr–9Ni alloy, and points to the difference in the nitriding mechanisms.

Fig. 2 shows the X-ray diffraction pattern at the specimen surface after removal of the surface layer to a depth of less than 0.1 μm, as measured by a digital micrometer. This specimen was quenched in cold water within 20 s of plasma nitriding at 823 K for 108.0 ks. Both CrN and the austenitic matrix phase were observed, but no iron nitride was detected. This

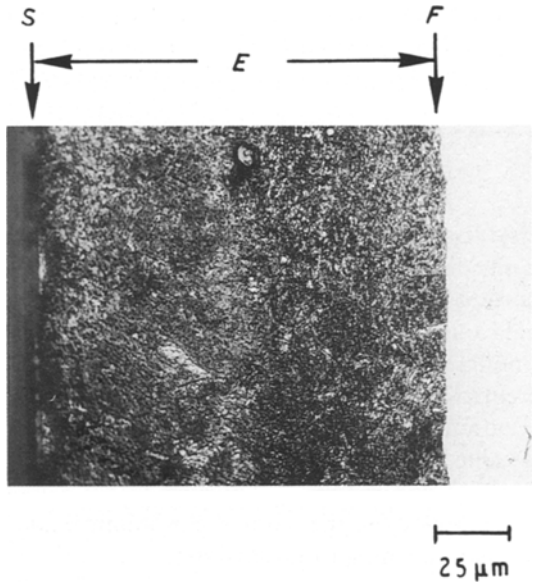

Figure 1 Typical microstructure of the Fe–18Cr–9Ni alloy nitrided by plasma at 823 K (550 °C) for 108 ks (30 h).

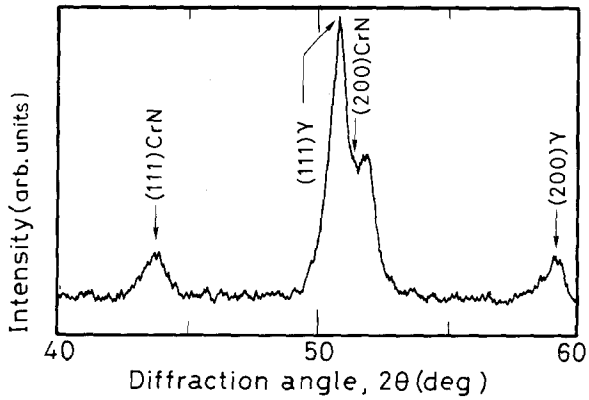

Figure 2 X-ray diffraction pattern at the specimen surface nitrided by plasma at 823 K (550 °C) for 108 ks (30 h). CoK_α was irradiated.

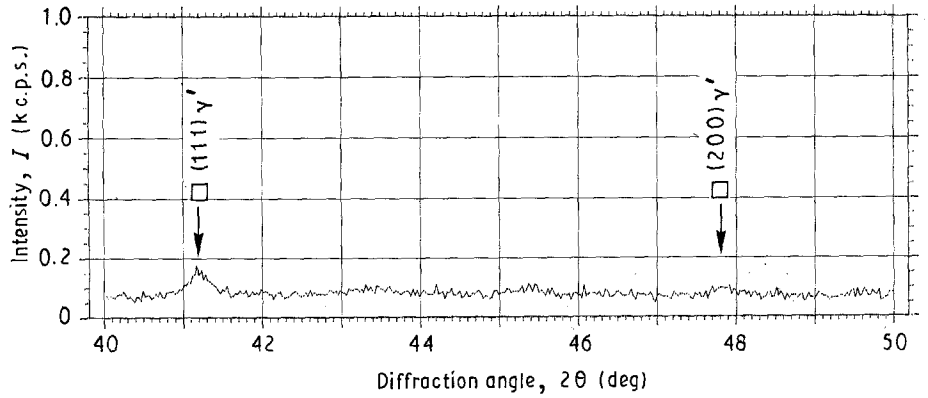

Figure 3 X-ray diffraction pattern at the surface of (1 0 0) Si which was set by Fe–18Cr–9Ni alloy during plasma nitriding. CuK_α was irradiated.

result is consistent with the microstructural observation shown in Fig. 1. The XRD result is markedly different from that obtained by ammonia gas nitriding. The external nitriding layer formed by the ammonia gas nitriding consisted mainly of γ'-Fe_4N and CrN [5]. Moreover, the precipitation of Cr_2N in the matrix of austenitic phase was detected in the nitriding layer formed by ammonia gas. On the other hand, the precipitation of CrN in the matrix of austenitic phase was detected throughout the nitriding layer formed by plasma nitriding. CrN is precipitated more stably than Cr_2N when it contains an adequately higher concentration of nitrogen [8]. Accordingly, plasma nitriding can adequately transfer nitrogen from the plasma to the solid. It is therefore apparent that the mechanism of plasma nitriding is different from that of ammonia gas nitriding.

Fig. 3 shows the XRD pattern at the surface of Si which was set by Fe–18Cr–9Ni alloy during plasma nitriding. The deposition of γ'-Fe_4N was clearly observed. This results from sputtering from the surface of the Fe–18Cr–9Ni alloy as soon as the γ'-Fe_4N was formed. Since the sputtering ratio of iron by Ne or Ar ions is nearly equal to those of chromium and nickel [9], iron as well as chromium and nickel may be sputtered by ions of the molecule species N_iH_j ($i = 1, j = 1$–5; $i = 2$, $j = 2$) during plasma nitriding [10]. However, only γ'-Fe_4N is clearly identified in Fig. 3. The results shown in Fig. 3 mean that γ'-Fe_4N is more readily sputtered than CrN. The iron nitride is less stable in plasma at 823 K than chromium nitride, since the formation energy of iron nitride, γ'-Fe_4N, is 26.17 kJ mol^{-1}, which is less than that of chromium nitride, CrN, $-$ 523.37 kJ mol^{-1} [11]. Accordingly, the plasma nitriding of Fe–18Cr–9Ni alloy does not result in the formation of an external nitriding layer. An internal nitriding layer, consisting of CrN and austenitic iron alloy, is, however, formed.

Fig. 4 shows the change in the lattice constant of the austenitic phase as a function of distance from the specimen surface. Each lattice constant is calculated from (3 1 1) diffraction of γ-Fe. It is well known that the lattice constant of the austenitic phase depends on the dissolved concentration of interstitial atoms [12–14]; the lattice constant increases with increased

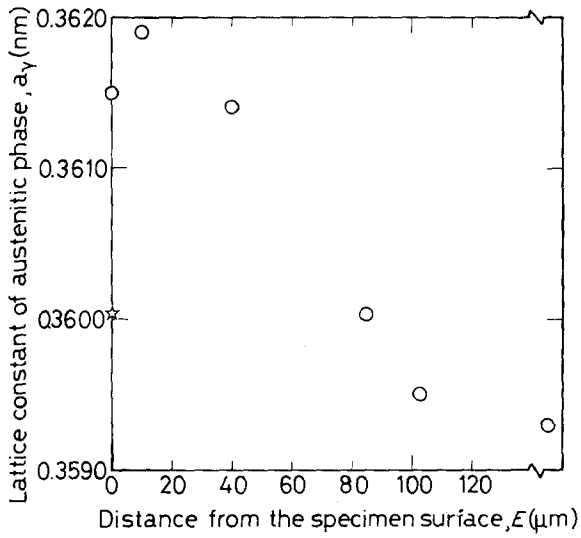

Figure 4 Relationship between the lattice constant of the austenitic phase and the distance from the specimen surface. The lattice constant was calculated from the (3 1 1) plane of austenitic phases. ☆ at the specimen surface nitrided by ammonia gas.

nitrogen concentration. However, the quantitative relationship between the lattice constant of the austenitic phase in equilibrium with CrN and the concentration of the dissolved nitrogen is not clear. We could not, therefore, determine the change of dissolved nitrogen with the distance from the specimen surface. In Fig. 4, the lattice constant at the specimen surface is smaller than at 10 μm from the surface. This indicates that the concentration of dissolved nitrogen at the specimen surface is lower than in the inner region—which ranges from 10–40 μm from the specimen surface. The collision of ion species affects not only the absorption of nitrogen but also its removal; that is, the plasma nitriding reaction advances with the breathing of nitrogen. If sputtering did not occur, the maximum concentration of dissolved nitrogen would be obtained at the specimen surface. This concentration profile is therefore ascribed to the sputtering.

Moreover, "☆" in Fig. 4 shows the lattice constant that was obtained by ammonia gas nitriding of the present alloy [5]. There, the concentration of dissolved nitrogen at the specimen surface is lower than that at the surface of the specimen nitrided by plasma.

That is, plasma nitriding introduces a larger amount of nitrogen into the solid alloy than gas nitriding.

5. Conclusions

Plasma nitriding of Fe–18Cr–9Ni alloy at a temperature of 823 K was carried out in order to clarify the role of the plasma in the plasma nitriding process. X-ray diffraction analysis was used to examine the nitrides at the nitrided specimen surface and at the surface of Si. Microstructural observations were made to study the formation of the nitriding layers. The main conclusions are as follows.

1. Plasma nitriding does not result in the formation of an external nitriding layer. Ions in the plasma sputter the iron nitrides as soon as they form.

2. The internal nitriding layer formed by plasma nitriding consists of both austenitic phase and CrN.

3. The lattice constant of the austenitic phase with dissolved nitrogen at the specimen surface is greater than that obtained by ammonia gas nitriding of Fe–18Cr–9Ni alloy.

Acknowledgement

The authors are indebted to K. Kimura for his help with X-ray diffraction work.

References

1. H. KUWAHARA, H. MATSUOKA, J. TAKADA and I. TAMURA, *J. Jpn. Plating Coating*, **10** (1990) 54.
2. Metals Handbook, Heat treating, edited by American Society for Metals 9th Edn, Vol. 4 (Metals Park, Ohio, 1981).
3. B. BILLON and A. HENDRY, *Surf. Eng.* **1** (1985) 114.
4. H. KUWAHARA, J. TAKADA and I. TAMURA in Proceedings of the 7th International Symposium on Plasma Chemistry, Eindhoven, July 1985, edited by C. J. TIMMERMANS (International Union of Pure and Applied Chemistry, Eindhoven, 1985). 473.
5. H. KUWAHARA, H. MATSUOKA, Y. TOMII, S. KIKUCHI, J. TAKADA and T. TAKAYAMA, *J. Mater. Sci.*, **25** (1990) 4120.
6. L. E. KINDLIMANN and G. S. ANSELL, *Metall. Trans.* **1** (1970) 163.
7. J. M. SILCOCK, *Metal Sci.* **14** (1978) 561.
8. B. MORTMER, P. GRIEVESON and K. H. JACK, *Scand. J. Metall.* **1** (1972) 203.
9. B. N. CHAPMAN in "Glow Discharge Processes: Sputtering and Plasma Etching" (John Wiley & Sons, Inc., New York, 1980)
10. M. HUDIS, *J. Appl. Phys.* **44** (1973) 1489.
11. Metals Data Book, edited by Japanese Society of Metals (Maruzen, Tokyo, 1974)
12. M. TSUCHIYA, M. IZUMIYAMA and Y. IMAI, *J. Jpn. Inst. Metal.* **29** (1965) 427.
13. G. FANINGER and A. FREIßMUTH, *Acta. Phys. Austrica*, **18** (1964) 280.
14. M. KIKUCHI, T. TANAKA, K. HAMAGAMI, Y. OGURA and R. TANAKA, *Metall. Trans.* **7A** (1976) 906.

Received 13 August 1990
and accepted 28 February 1991